Energy Efficiency Analysis of Natural Convection Heat Transfer in Concentric Annulus with Interior and Exterior Grooves

KHAOULA BEN ABDELMLEK, FAYÇAL BEN NEJMA
[1]Laboratory Studies of Ionized and Reactive Media,
University of Monastir,
Road Ibn Eljazzar, 5019 Monastir,
TUNISIA

Abstract: - This study is a numerical investigation of the convective heat transfer in motionless concentric annulus composed of two horizontal cylinders, one of which is grooved. The inner cylinder is kept at hot temperature T_h and the outer one is kept at cold temperature T_c. The aim of this paper is to analyze the effect of the groove on thermal and dynamic behavior in the annulus when the groove is located on the hot cylinder (inner groove), and when it is located on the cold cylinder (exterior groove). To observe the effect the inner and outer groove on the flow structure and on the heat transfer rate, the groove is positioned at ϕ_0=-90°, -45°, 0°, 45°, and 90°. Moreover, the groove size (f) and the radius ratio (e) of the annulus have been changed to investigate their effects on heat transfer rate as well as on the energy efficiency of the process. The results show that the heat transfer rate rises up with the increase of Rayleigh number. It is seen that; in the case of the inner groove; the heat transfer rate reaches a maximum at ϕ_0=40°, whatever the groove size. Furthermore, the energy efficiency of the process is maximum when the inner groove is positioned at ϕ_0=90°, and it increases well with the increase of f. On the other hand, in the case of the exterior groove, the heat transfer rate is practically close to that of non-grooved annulus for f<0.7. A decrease of 34% of the energy efficiency is noticed with the increase of the size of the groove to f=0.7. Our results would be very useful for manufacturers who are looking for increasing the energy efficiency of their process, or also who need to boost or decrease the heat transfer rate depending on the objective of their process.

Key-Words: - Interior grooved pipe, exterior grooved pipe, energy efficiency, heat transfer rate, natural convection, groove position, radius ratio, groove size.

Received: March 28, 2023. Revised: September 12, 2023. Accepted: November 2, 2023. Published: December 12, 2023.

1 Introduction

Although the natural convection heat transfer in concentric, [1], [2], [3], [4], [5], [6], [7], and eccentric annulus, [8], [9], [10], is widely explored in the literature, it is still the subject of several recent works, thanks to its importance and its impact on the energy efficiency and the performance of many modern technologies including cooling of electronic components, solar heating, heat recovery applications, underground storage etc. We could see some major examples in the literature about the control of thermal behavior and fluid flow in annulus as can be seen below.

Natural convection heat transfer in motionless concentric annulus filled with air was treated by, [11]. Special attention was paid to the thermo convective instabilities in the annulus. [12], investigated the effect of eccentricity on dynamic behavior. [13], tested the effect of fluid properties using CO_2 in the annular space. They explored its impact on dynamic and thermal properties in Couette flow. A large number of research works were also investigated to study convective heat transfer in concentric and eccentric annulums considering various boundary conditions: isothermal, [14], [15], and constant heat flux, [16]. Other research works are rather focused on highlighting the effect of eccentricity, radius ratios, dimensionless numbers on the convective heat transfer rate in the annulus, [17], [18].

The shape of the annulus has certainly a considerable effect on the rate of convective heat exchange. This has been the subject of recent research works. They have focused on the study of natural convection in an annulus whose interior cylinder is elliptical, [19], rectangular, [20], triangular, [21], or even grooved cylindrical, [22], [23], [24], [25], since in many fluid transport applications, the flow must pass through grooved cylindrical pipes. Several research works have been developed in this dynamic to study the effect of the groove on the flow pattern, [22], studied using the

particle image velocimetry (PIV) method the case of flow around cylinders containing rectangular grooves. The effects of groove position and size were then explored and the authors showed that wake flow structure is largely affected by groove position. However, the frequency of Karman vortex shedding depends rather on the size of the groove. Subsequently, the same authors, [23], studied experimentally the case of square-shaped grooves. The pipe under study was positioned at different groove angles in the water using the PIV method. They detected then that the critical position of the groove that triggers the start of flux separation is 80°. [24], compared flows around different groove shapes on cylinders: They determined through their experimental work the highest and lowest drag coefficient for the studied grooves. In our previous work, [25], we studied the convective transfer around a hot grooved cylinder in a cold rectangular cavity. We then developed a comparison between two shapes of groove: triangular and circular grooves. The effects of the size and position of the groove on the temperature and velocity profiles as well as on the heat transfer rate in the cavity were studied.

With the advent of industrial advancement, the continuation of research and studies of convective heat transfer must meet the requirements of recent environmental and industrial applications in terms of improving thermal performance and energy efficiency of processes. In this context, [26], [27], studied numerically the case of concentric and eccentric annulus respectively. The inner cylinder is supposed to be hot and rotating, however the outer one is cold and immobile. The effect of Rayleigh number, eccentricity, rotational speed of the inner cylinder was numerically investigated on the energy efficiency of the annulus. They showed that maximum energy efficiency is achieved with higher Rayleigh numbers as well as with small eccentricity.

[28], developed numerically an analysis of free convection in a horizontal cylinder partially heated at various locations on its sidewalls. The effects of heat source location on the flow pattern as well as on the heat transfer rate were investigated. The authors proved then that the heating process is more efficient when the heat source is located on the top of the cylinder. The results obtained may be very useful for various heating/cooling process applications.

Through the review of the literature cited above, we notice that, for the case of grooved annulus, the authors focused on the dynamic behavior around grooved pipes. But, less attention is paid to the analysis of the thermal characteristics of the fluid in the grooved pipes. In fact, the transport of fluids in pipes requires, depending on the intended application, the reduction of heat losses to maintain a constant temperature of the transported fluid, or also the maximization of heat transfer if it is a fluid cooling application. Add to that, improving the energy efficiency of the process is becoming a major challenge for manufacturers. Whatever the industrial sector, it is now essential to boost the profitability and efficiency of the process in terms of energy.

In this context, and as a continuation to our previous work, [25], we propose in this paper to study the heat transfer by natural convection in a grooved concentric annular space. The inner cylinder is kept hot while the outer one is cold. In the first part of this paper, the groove is placed on the hot cylinder, and it is at the level of the outer cylinder in the second part of this manuscript. The effect of the radius ratio of the annulus, the groove location and size on the heat transfer rate, the fluid flow pattern as well as on the energy efficiency of the process are highlighted in this numerical study for the case of interior and exterior groove.

2 Mathematical Modeling

2.1 Problem Formulation

Figure 1 illustrates schematically the geometry of the proposed numerical model to be treated in this study. It is composed of two horizontal cylinders between which circulate a laminar and incompressible fluid flow. The inner cylinder of radius R_{in} is maintained at a hot temperature of T_h while the outer cylinder of radius R_{ex} is kept isothermal at a cold temperature T_c. Two cases of groove are analyzed in this study: the case where the inner pipe is grooved, and the case where the groove is at the level of the outer pipe. The interior groove is obtained from the difference between two cylinders of radius R_{in}. One of the cylinders is positioned at a distance of $2.f.R_{in}$ from the other one as illustrated in Figure 2. The difference between these two cylinders provides a grooved duct. Similarly, to obtain the exterior groove on the annulus, it suffices to subtract from the latter a cylinder of radius R_{ex} positioned at a distance equal to $2.f.R_{ex}$ from the outer cylinder. As shown in Figure 2, the groove location is then defined by the angle φ_0.

The effect of Rayleigh number, the radius ratios e, the groove location φ_0 and its size f, on the dynamic and thermal distributions as well as on the

amount of heat transferred and the energy efficiency in the annulus are tested in this work for the case of interior and exterior groove. It should be noted that the position of the groove is determined by the angle φ_0 between its center and the axis (Ox).

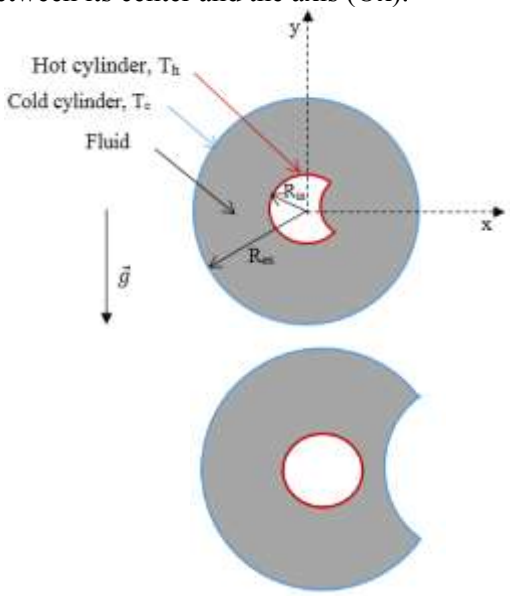

Fig. 1: Schematic geometry of the problem for the case of interior groove and exterior groove

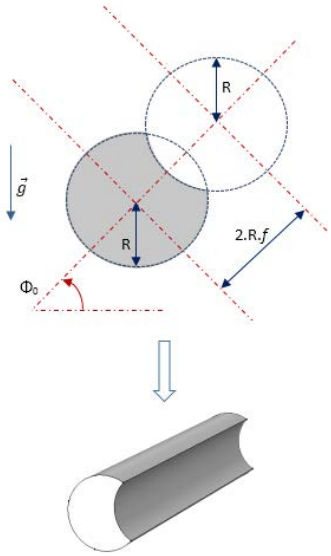

Fig. 2: Schematic representation of the grooved pipe

2.2 Assumptions and Governing Equations

The following assumptions are made to simplify the numerical modeling:

- The temperature and the flow profiles are assumed bidirectional.
- The fluid is Newtonian and the flow field is steady, laminar and incompressible.
- Pr= 0,71.

Considering these assumptions, the governing equations in dimensionless form are written in Cartesian- coordinates system as below:

$$\frac{\partial U}{\partial X}+\frac{\partial V}{\partial Y}=0 \quad (1)$$

$$U\frac{\partial U}{\partial X}+V\frac{\partial U}{\partial Y}=-\frac{\partial \Pi}{\partial X}+\mathrm{P}_r\left[\frac{\partial^2 U}{\partial X^2}+\frac{\partial^2 U}{\partial Y^2}\right] \quad (2)$$

$$U\frac{\partial V}{\partial X}+V\frac{\partial V}{\partial Y}=-\frac{\partial \Pi}{\partial Y}+\mathrm{P}_r\left[\frac{\partial^2 V}{\partial X^2}+\frac{\partial^2 V}{\partial Y^2}\right]+\mathrm{P}_r R_a \Theta \quad (3)$$

$$U\frac{\partial \Theta}{\partial X}+V\frac{\partial \Theta}{\partial Y}=\left[\frac{\partial^2 \Theta}{\partial X^2}+\frac{\partial^2 \Theta}{\partial Y^2}\right] \quad (4)$$

where the non-dimensional groups used in this numerical study are as follows: $X=\frac{x}{R_{ex}}$; $Y=\frac{y}{R_{ex}}$; $r=\sqrt{X^2+Y^2}$; $U=\frac{uR_{ex}}{\alpha}$; $V=\frac{vR_{ex}}{\alpha}$; $\Theta=\frac{T-T_c}{T_h-T_c}$; $\Pi=\frac{PR_{ex}{}^2}{\rho\alpha^2}$; $\mathrm{Pr}=\frac{\nu}{\alpha}$; $Ra=\frac{g\beta}{\nu\alpha}R_{ex}{}^3\Delta T$

The local Nusselt number of interior and exterior pipes is calculated as follows:

$$Nu_{in,ex}=2.\left|\frac{\partial \Theta}{\partial X}.n_x+\frac{\partial \Theta}{\partial Y}.n_y\right|_l \quad (5)$$

Where n_x and n_y are the components of the normal to the grooved surface

The average Nusselt number is determined as follows:

$$Nu=\frac{1}{L}\int_0^L Nu_l\,dl \quad (6)$$

Where l and L are respectively the position and the total length of the grooved surface.

To improve the efficiency of the heating process we define the energy efficiency as follows:

$$\varepsilon=\frac{\Theta_a}{f.Nu_{\mathrm{in}}} \quad (7)$$

2.3 Boundary Conditions

a) For the inner cylinder: u=0, T=Th
b) For the exterior cylinder: u = 0, T=Tc

2.4 Numerical Procedure and Validation

A computational fluid dynamics (CFD) code named COMSOL Multiphysics® software and based on finite element method is used to discretize and solve the partial differential equations in the grooved annular space. The resolution of the numerical problem is carried out using an implicit scheme based on Newton's method (damping factor equal to 0.8). The used mesh depicted in Figure 3 is composed of triangular elements and it is refined close to the wall where the temperature and velocity gradient are high.

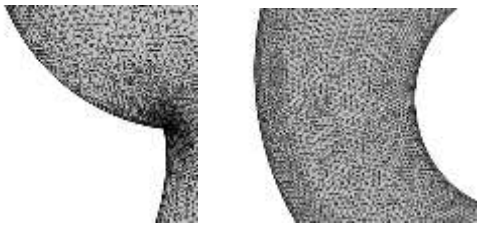

Fig. 3: Grid resolution of the numerical model on COMSOL

To check the validity of our numerical code, we treated the case of non-grooved cylindrical annulus differently. The inner cylinder is hot; however, the outer one is cold. The flow is assumed to be laminar and incompressible. We compared our numerical results in terms of convective heat transfer rate (Nu_{in} values) on the inner cylinder with those of [20], for different Rayleigh numbers (Table 1). The agreement seems to be satisfying, and the percentage of simulation error justifies that our numerical model can perfectly predict the thermal and dynamic behaviour in the grooved annulus.

Table 1. Comparison between the Nu_{in} values of this study and those of ref [10]

Ra	**10^3**	**10^4**	**5.10^4**
Nu_{in} of reference[10]	1.11	2.00	3.03
Nu_{in} [present work]	1.08	1.98	2.98
% simulation error	2.77	1	1.65

3 Results and Discussions

Numerical simulations were performed for Pr=0.71, and different values of Rayleigh number in the range between 10^3 and 10^6. To provide better understanding of the parametric study, we highlight; for both exterior and interior groove; the effect of groove location Φ_0, groove size f, and radius ratio e on local distributions of temperature and velocity as well as on the heat transfer rate and the energy efficiency of the heating process.

3.1 Interior Groove

3.1.1 Effect of the Groove Location

Figure 4 and Figure 5 illustrate temperature and velocity profiles as well as local distributions of interior and exterior Nusselt numbers respectively for Ra=10^5 and different groove locations.

The hot fluid rises above the hot cylinder in the annular space due to the density difference, following an ascending thermal plume for all groove locations. Two counter-rotating cells are developed on either side of the hot inner cylinder. They contain recirculation, which changes locations by changing the position of the groove. What is remarkable here is that the evolution of Nu_{ex} is not affected by the position of the groove. Indeed, the temperature gradient is maximum at the top of the cold outer cylinder, which maximizes the convective transfer rate and explains the maximum value of Nu_{ex} in this part. Moreover, we note a stagnant fluid region at the bottom part of the annulus whatever the groove position. In fact, the temperature difference between the fluid and the outer duct is very low. This leads to a slow-down of the heat transfer amount there.

By analyzing the heat transfer around the hot cylinder for different groove locations studied, we note that the thickest thermal boundary layer is located on the grooved surface. This reduces the amount of heat exchanged and explains the decrease in Nu_{in} in the grooved part except its ends, where the heat transfer is maximum since the temperature gradient is high.

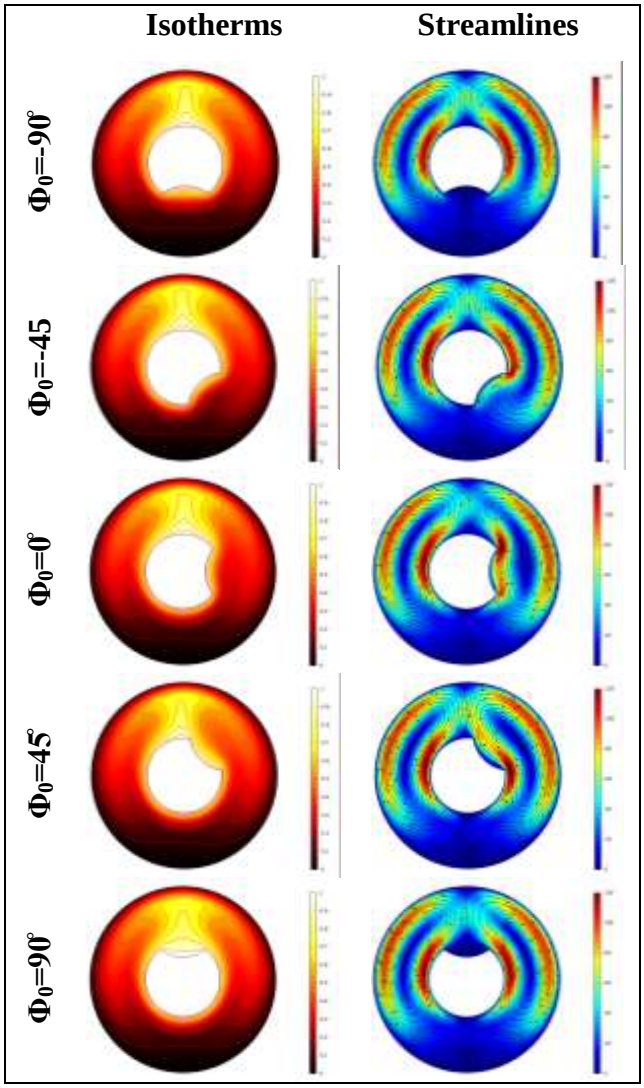

Fig. 4: Isotherms and streamlines for different inner groove locations, e=0.4, f=0.8, Ra=1E5

3.1.2 Effect of Groove Size

Figure 6 and Figure 7 illustrate variations of dimensionless temperature, velocity and Nusselt numbers respectively in the annulus for different groove sizes f.

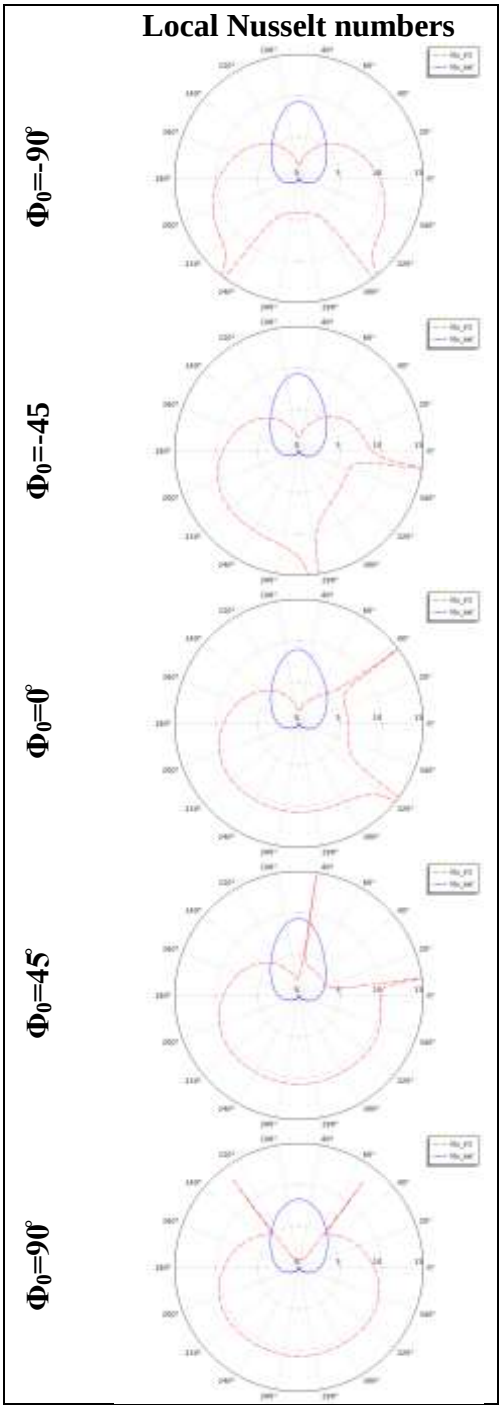

Fig. 5: Evolution of local Nusselt numbers for different inner groove locations, e=0.4, f=0.8, Ra=1E5

For non-grooved pipe f=1, the temperature and velocity profiles are perfectly symmetrical with respect to the vertical median. Thermal boundary layers are developed on the totality of the hot cylinder, thus promoting heat transfer from the inner cylinder to the fluid in the annulus. The thermal plume is directed vertically upwards, promoting then heat exchange on the top of the outer cylinder. The fluid particles in the bottom part of the annulus are practically motionless and the transfer rate is almost zero on the cold cylinder.

In return, it is maximum on the inner cylinder given the strong temperature gradient between the hot pipe and the stationary fluid. By creating interior grooves (f=0.9), we remark that the thickness of the thermal boundary layer increases on the groove region. This explains the drop in the heat transfer rate and the reduction in Nu_{in} in this zone. The latter reaches maximum values at the ends of the grooved surface since the temperature difference is maximum there. By further increasing the size of the groove, the amount of exchanged heat remains almost constant on the outer and inner pipe except for the grooved part where Nu_{in} decreases. Moreover, the maximum values of Nu_{in} are similarly detected at the extremities of the grooved surface and they increase by increasing the size of the groove thanks to the amelioration of the temperature gradient.

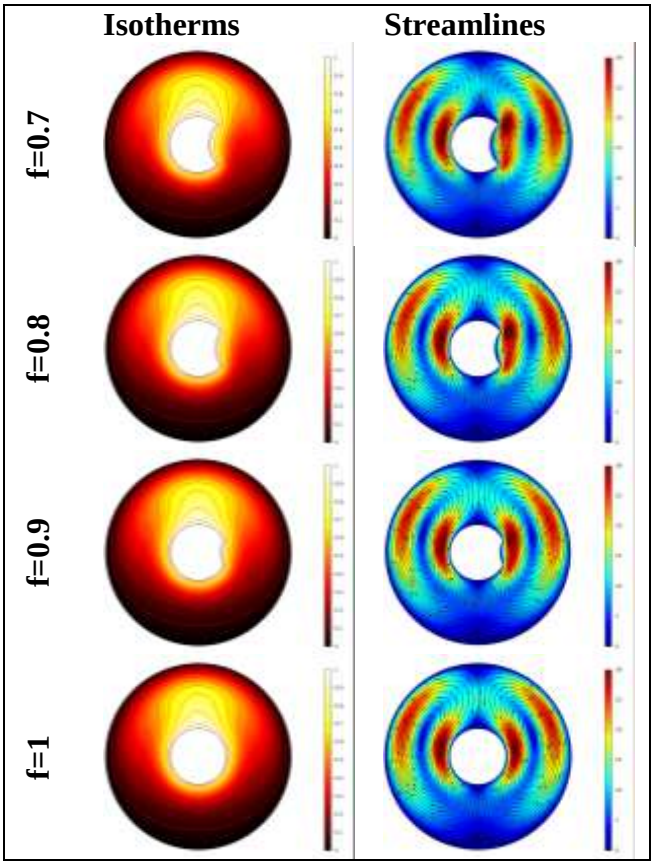

Fig. 6: Isotherms and streamlines for different inner groove sizes, e=0.3, ϕ0=0°, Ra=1E4

The evolution of mean dimensionless temperature as a function of the groove location ϕ_0 is presented in Figure 8. We note here that the average temperature of the annular space increases by changing the position of the groove ϕ_0 in the counter-clockwise direction whatever the size of the groove. Furthermore, it should be noted that when $\phi_0 \in$ [-90°, 65°], the average dimensionless temperature reaches its maximum value in the absence of the groove and decreases with increasing groove size f. On the other hand, when ϕ_0 is on the interval [65°, 90°], the mean dimensionless temperature rises with increasing size of the groove f. Thus, the case ϕ_0 =65° presents a critical case where the average temperature becomes constant and is no longer affected by the presence of the groove and its size.

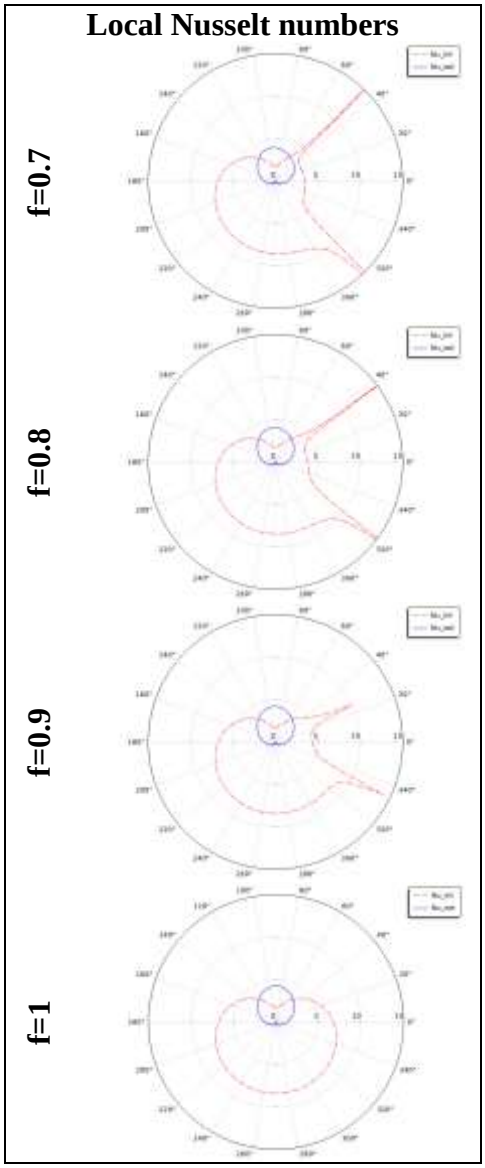

Fig. 7: Evolution of local Nusselt numbers for different inner groove sizes, e=0.3, ϕ_0=0°, Ra=1E4

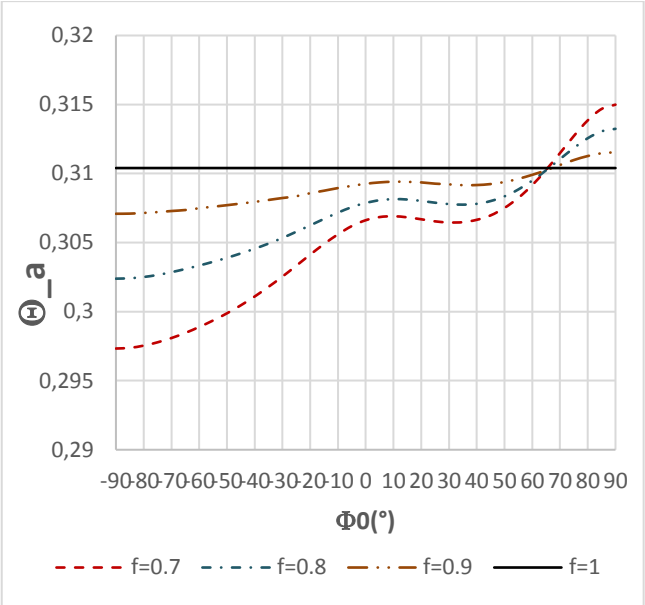

Fig. 8: Effect of inner groove size on the mean dimensionless temperature

The influence of the groove location on the heat transfer rate is given in Figure 9 for different groove size f. As shown, in the presence of the groove, the profile of Nu_a initially shows an increasing trend reaching a maximum when the groove is placed at about 40° from the horizontal. Then, the heat transfer rate decreases when the groove location is on the range [40°,90°].

Figure 10 illustrates the impact of the groove position on the energy efficiency of the heating process. It is worth noting that the evolution is sinusoidal and there are groove locations that limit the energy efficiency of the process. In fact, according to the curve, for the two locations ϕ_0=-50° and ϕ_0=40°, the heat transfer process is the least efficient. On the other hand, the curve of the energy efficiency presents two maximum values obtained when the groove is positioned at an angle ϕ_0=0° and ϕ_0=90° regardless of its size.

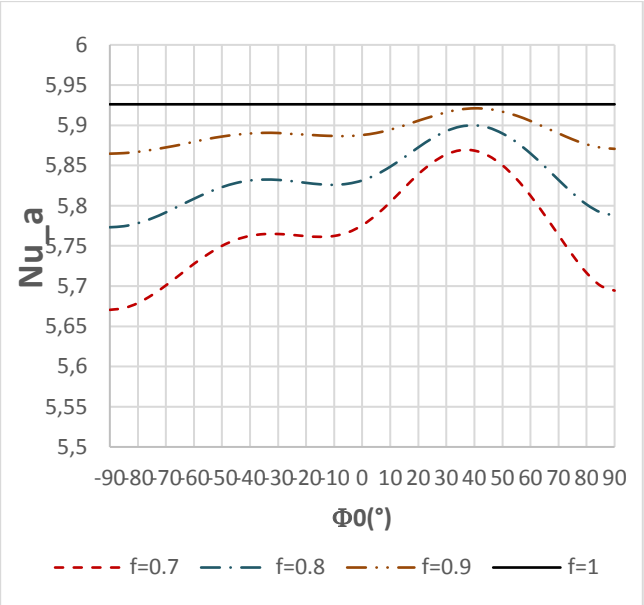

Fig. 9: Effect of inner groove size on the average Nusselt number

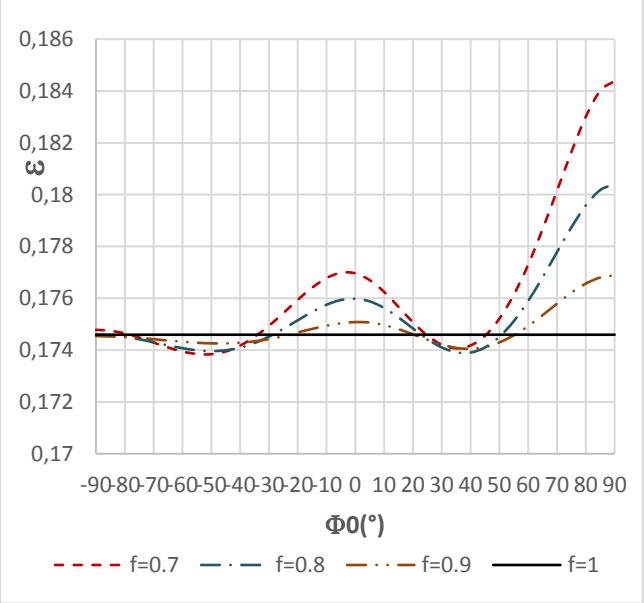

Fig. 10: Effect of inner groove size on the energy efficiency of the process

3.1.3 Effect of Rayleigh Number

The evolutions of local distributions of dimensionless temperature and velocity with regards to Rayleigh number are reported in Figure 11. It can be seen that for lower Rayleigh numbers, the heat is totally transferred by conduction. The temperature gradient is very low in the vicinity of the outer cylinder, which inhibits the heat transfer rate and explains the lower values of Nu_{ex} in this region as illustrated in Figure 12. Two counter rotating cells are developed on both sides of the inner cylinder and contain secondary recirculation, which change locations by increasing the Rayleigh number.

Noteworthy here is that the thermal plume starts to appear with $Ra=10^4$. The hot fluid is rising above the inner cylinder, increasing the temperature gradient in the upper part of the annulus and promoting the amount of heat exchange. Furthermore, the thickness of thermal boundary layers developed around the inner hot cylinder drop with the increase of the Rayleigh number. This results in an amelioration of the heat transfer rate which achieves its maximum values at the extremities of the grooved part.

For $Ra=10^5$, a stagnant fluid zone is noticed in the lower part of the annular space. On the other hand, the flow circulation accelerates in the rest of the domain since the plume is fully developed. The Nu_{ex} values are then practically zero in the stagnation zone and they are maximum at the plume level. It should also be noted that the temperature gradient improves more around the inner cylinder for $Ra=10^5$. This explains the improvement of the Nu_{in} which reaches its maximum values at the extremities of the groove where the flow velocity is maximum.

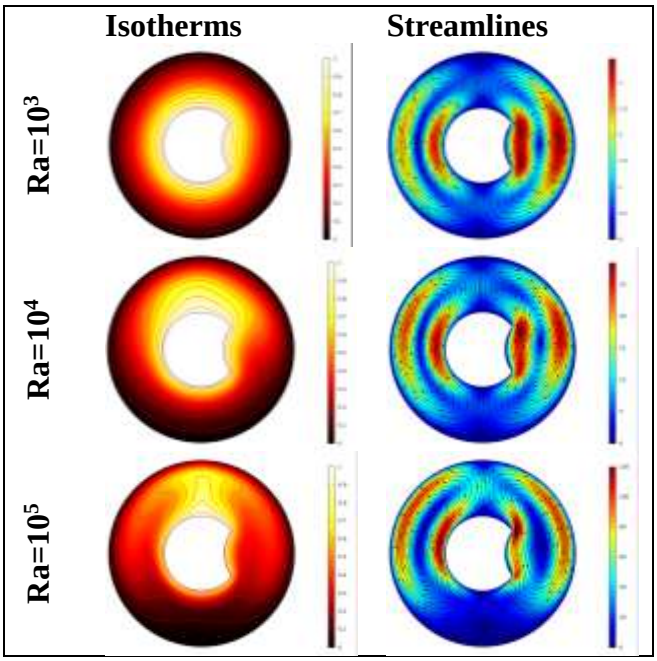

Fig. 11: Isotherms and streamlines for different Rayleigh numbers for the case of inner groove, e=0.4, $\phi_0=0°$, f=0.8

The effect of the Rayleigh number on the evolution of the dimensionless temperature in the annulus is illustrated in Figure 13. It is quite obvious that the dimensionless temperature remains almost constant for low Rayleigh number ($Ra=10^3$) since the transfer is only by conduction. By increasing the Rayleigh number, the dimensionless

temperature values decrease and describe an increasing profile as a function of the groove orientation angle.

Furthermore, as shown in Figure 14, the rate of heat transfer increases as a function of the Rayleigh number. On the other hand, the rate is practically constant by changing the position of the groove. As for the energy efficiency of the process, it can be seen in Figure 15 that it decreases with increasing Rayleigh number, and it is not affected by the position of the groove.

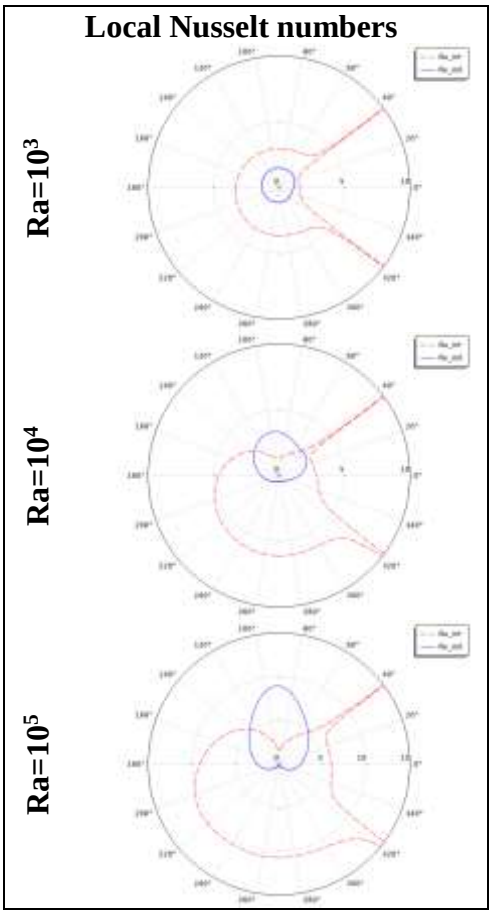

Fig. 12: Evolution of local Nusselt numbers for different Rayleigh numbers for the case of inner groove, e=0.4, ϕ_0=0, f=0.8

3.1.4 Effect of the Radius Ratio

The effects of radius ratio on local distributions of dimensionless temperature, fluid flow and heat transfer rate are shown in Figure 16 and Figure 17 respectively. The fully developed thermal plume with a radius ratio e=0.4 shown in Figure 6 starts to decrease as the radius ratio increases, and disappears completely from a radius ratio e=0.6. This causes a slowing down of the heat transfer rate with the outer cylinder. In addition, the number of counter rotating cells decreases as e increases with a clear deceleration of their velocity due to the reduction of the annulus. The temperature gradient between the inner hot cylinder and the annular space then decreases, and leads to a decrease of the Nu_{in} values with the decrease of the exchange surface.

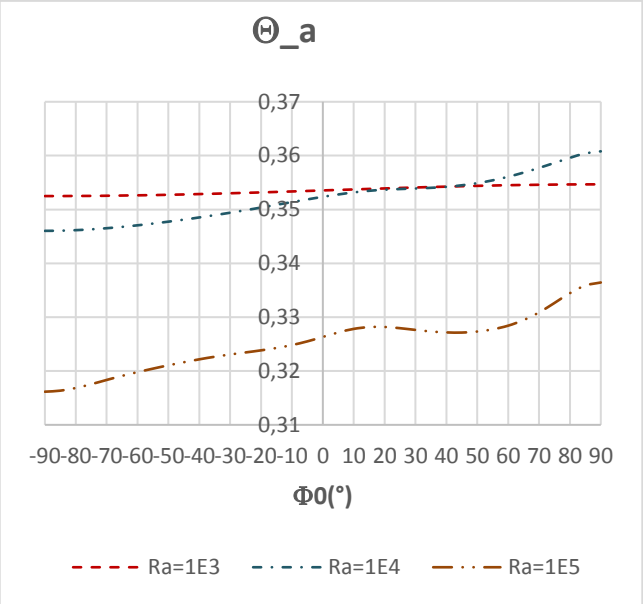

Fig. 13: Effect of Rayleigh number on the mean dimensionless temperature for the case of inner groove

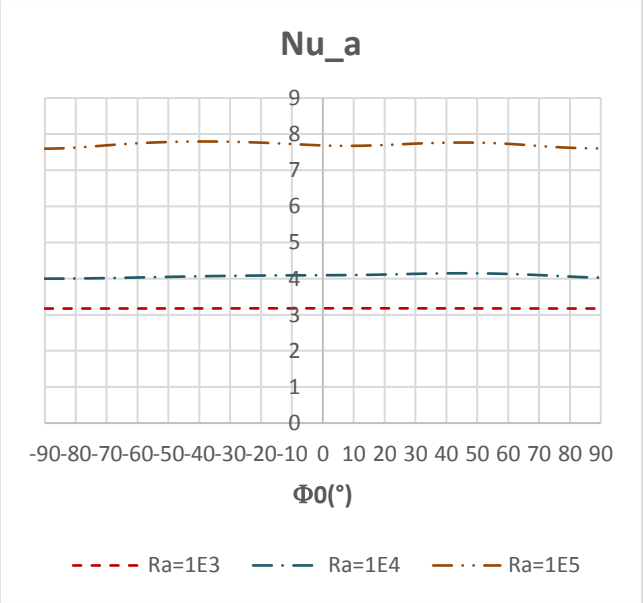

Fig. 14: Effect of Rayleigh number on the average Nusselt number for the case of inner groove

The evolution of the dimensionless temperature and heat transfer rate around the grooved cylinder as a function of the groove position are shown in Figure 18 and Figure 19 respectively for different radius ratios e.

Noteworthy here is that the dimensionless temperature in the annulus does not depend on the

position of the groove for the different radius ratios tested in this study. This provides a constant heat transfer rate in the annulus regardless of the groove position. On the other hand, by decreasing e, the exchange surface decreases, and the amount of heat exchanged also decreases, which leads to an increase in the dimensionless temperature of the process.

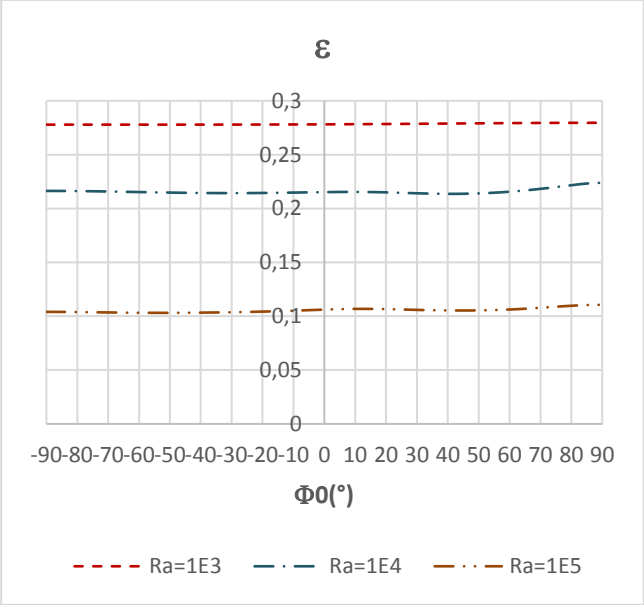

Fig. 15: Effect of Rayleigh number on the energy efficiency of the process for the case of inner groove

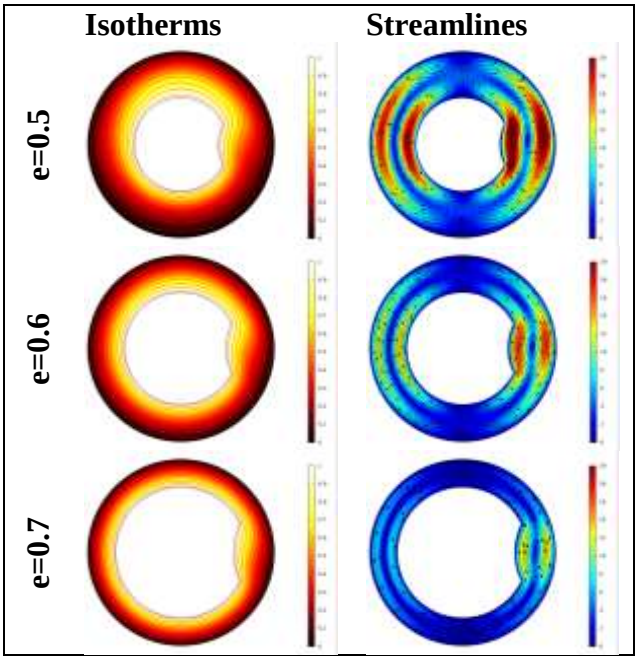

Fig. 16: Isotherms and streamlines for different radius ratios for the case of inner groove, $\phi 0=0$, f=0.9, Ra=1E4

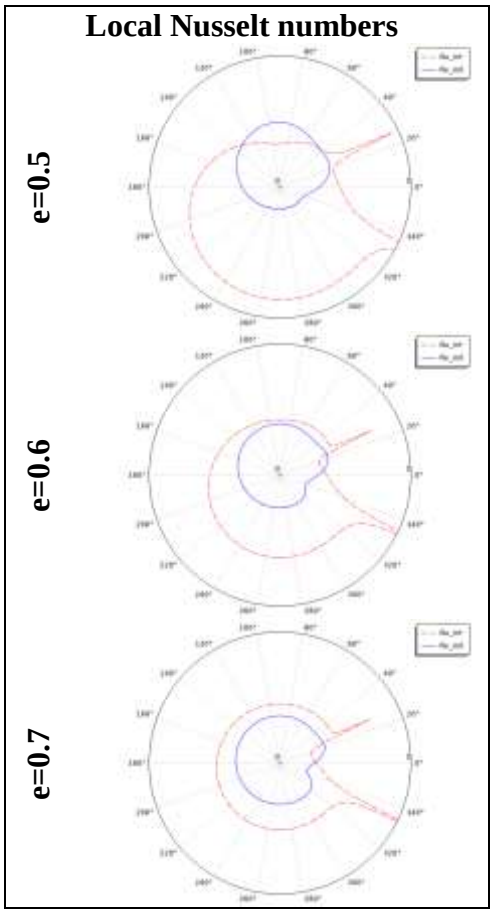

Fig. 17: Evolution of local Nusselt numbers for different radius ratios for the case of inner groove, $\phi_0=0$, f=0.9, Ra=1E4

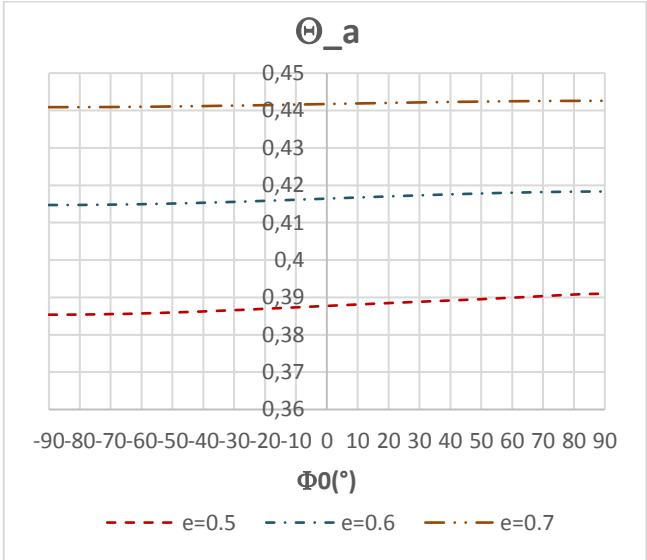

Fig. 18: Effect of radius ratio on the mean dimensionless temperature for the case of inner groove

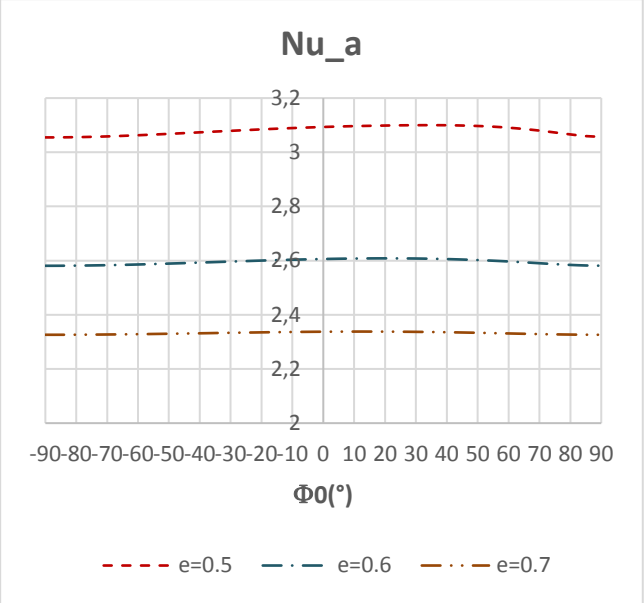

Fig. 19: Effect of radius ratio on the average Nusselt number for the case of inner groove

The effect of the radius ratio on the energy efficiency of the process is given in Figure 20 for different positions of the groove. We note that the energy efficiency remains almost constant when changing the groove position. A slight improvement is noticed on the interval [40°,90°] to reach maximum efficiency with a groove position ϕ_0=90° whatever the radius ratio. Moreover, the curve shows that the thermal system is more efficient by decreasing the annular space (high radius ratio), and its efficiency becomes stable from a radius ratio equal to 0,6.

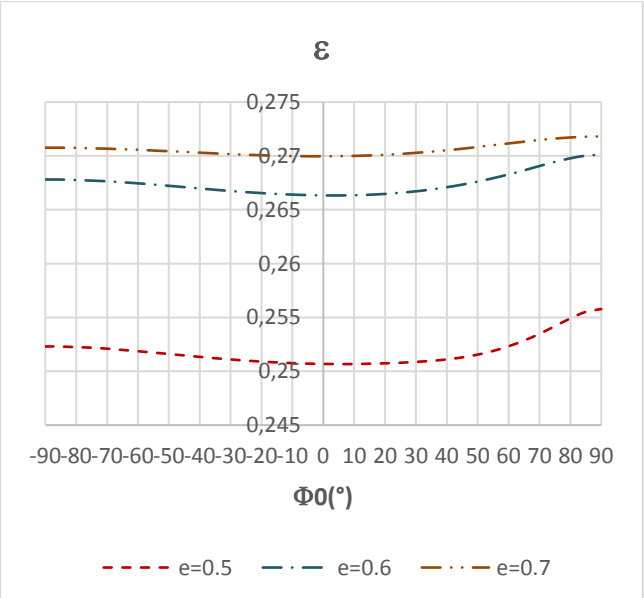

Fig. 20: Effect of radius ratio on the energy efficiency of the process for the case of inner groove

3.2 Exterior Groove

3.2.1 Effect of the Groove Position

Figure 21 and Figure 22 illustrate local distributions of dimensional temperature, velocity, interior and exterior Nusselt numbers in the annulus for different exterior groove positions.

When the groove is placed at the bottom of the annular space at an angle $\phi_0 = -90°$, the fluid flow presents two counter-rotating convective cells which are perfectly symmetrical with respect to the vertical median of the domain. The vertical thermal plume rising above the hot inner cylinder favors the heat exchange with the outer cylinder due to the presence of a strong temperature gradient. The values of Nu_{ex} are then maximum in this region. In addition, the thermal boundary layers developed around the inner cylinder create a temperature difference between it and the fluid particles in the annulus. This boosts the heat transfer rate around the hot cylinder except for its upper part where the thermal plume is fully developed. Note also that the presence of the external groove reduces the surface area at the bottom of the annular space. This improves the temperature gradient between the central part of the groove and the hot fluid around the inner cylinder. The value of Nu_{ex} is then high at the middle of the groove.

By changing the position of the groove to $\phi_0 = -45°$, the local distributions lose their symmetries. The left rotating cell becomes the most dominant and the thermal plume starts to deviate from the vertical median. The heat transfer rate with the hot inner cylinder is then maximal at the lower left part of the annular space where the temperature gradient reaches its maximum value. Furthermore, the local Nu-ex distribution shows that the heat transfer rate is maximum above the thermal plume. At the groove level, it should be noted that the thermal boundary layers developed around the hot cylinder are very close to the center of the groove due to the reduction of the annular space. This improves not only the temperature gradient in this region, but also the heat transfer rate with the outer grooved cylinder.

By moving to the position $\phi_0 = 0°$ and $\phi_0 = 45°$, the fluid flow is divided into three rotating cells. In fact, the presence of the groove on the right side of the annulus causes the deviation of the left cell and the division of the right cell into two.

In the two cases mentioned, we note a stagnation zone on the lower part of the annular space. This allows an excellent thermal exchange with the hot cylinder and on the other hand a very low transfer rate with the grooved cold cylinder. We also note

here that the fission of the right cell contributes to the intensification of the heat transfer rate with the external cylinder in this region following the increase of the thermal gradient there.

As shown in Figure 21, the position of the groove $\phi_0 = 90°$ causes a change of the local flow and temperature distributions in the annular space. In fact, the fluid flow acquires again its symmetrical aspect with respect to the vertical median. Two thermal plumes are developed in the upper part of the annular space. This leads to the formation of two counter-rotating cells, which dominate the annular space with the presence of a dead fluid zone in the form of two immobile cells near the center of the groove. The latter promotes the exchange with the hot cylinder.

3.2.2 Effect of Groove Size

The effect of the groove size on the local distributions of temperature, fluid flow and Nusselt numbers are highlighted in Figure 23 and Figure 24. What is remarkable here is that the thermal plume tilted to the left side with low f begins to deviate towards the vertical position as f increases. In addition, we notice that the annular space increases on the surface, which causes a decrease in the number of recirculation on the right side and an increase in the size of the left cell. This leads to an improvement in the flow velocity on this side. Finally the flow resumes its symmetrical aspect in the absence of the groove (f=1), following two rotating cells.

The heat transfer rate on the outer cylinder, which reaches maximum values at the middle of the grooved surface (due to the increase of the thermal gradient at the level of the groove), starts to fall as f increases. The result found is predictable since the circulation of the fluid is improved by increasing the exchange surface. On the other hand, the heat exchange with the hot cylinder increases on the right side, since the circulation of the fluid is improved by increasing the exchange surface. Note also that in the case of a low size groove (f=0.9) the amount of energy exchanged is almost identical to the case of a non-grooved cylinder.

Figure 25 shows the evolution of the average dimensionless temperature as a function of the position and size of the groove. For a groove located at an angle ϕ0=(-90°,-55°), the effect of its size is negligible. Indeed, whatever the size of the groove, the average dimensionless temperature in the annular space is slightly higher than in the case of non-grooved pipes. Above ϕ0=-55°, the size of the groove starts to have a considerable effect on the average temperature of the fluid.

According to the curve, large grooves (low f) lead to lower average temperatures. Moreover, in this case, the average temperature is very sensitive to the position of the groove. Indeed, we notice that the slope of the curve increases with decreasing f. By reducing the degree of the groove, the effect of its position decreases as the slope of the curve decreases, and the values of the average temperature of the fluid increase progressively approaching the values of the case f=1.

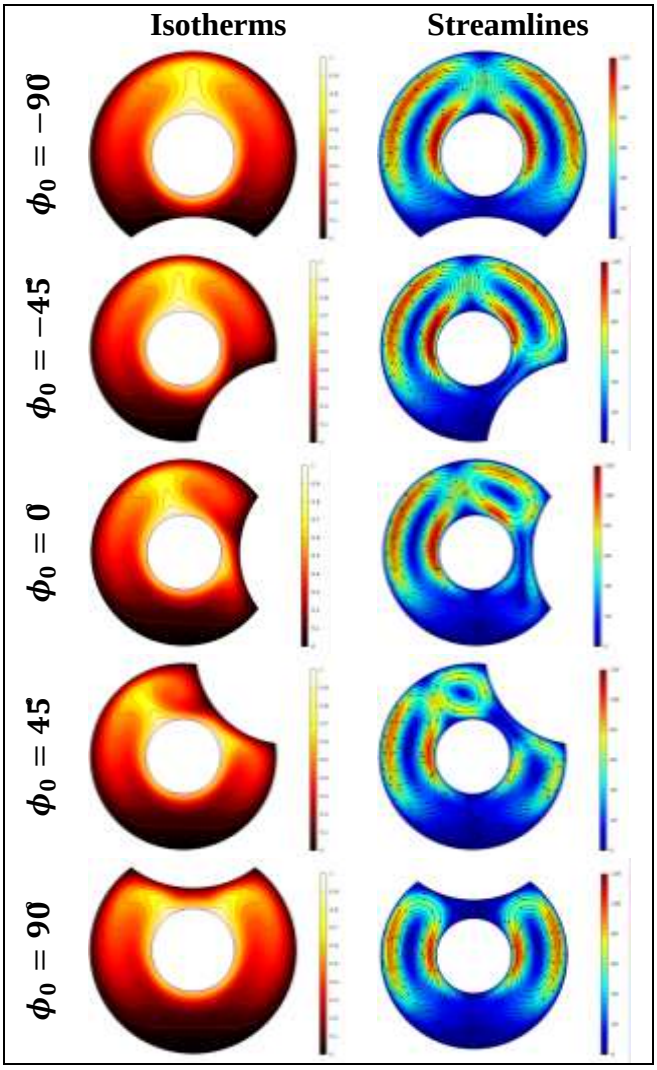

Fig. 21: Isotherms and streamlines for different exterior groove locations, e=0.4, f=0.8, Ra=1E5

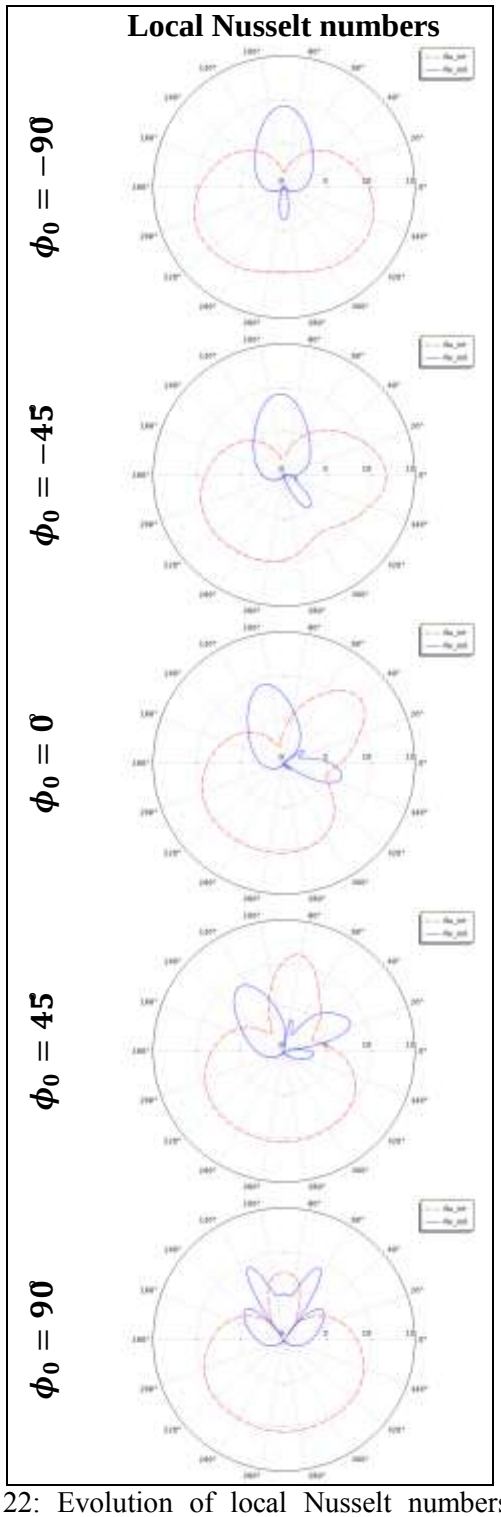

Fig. 22: Evolution of local Nusselt numbers for different exterior groove locations, e=0.4, f=0.8, Ra=1E5

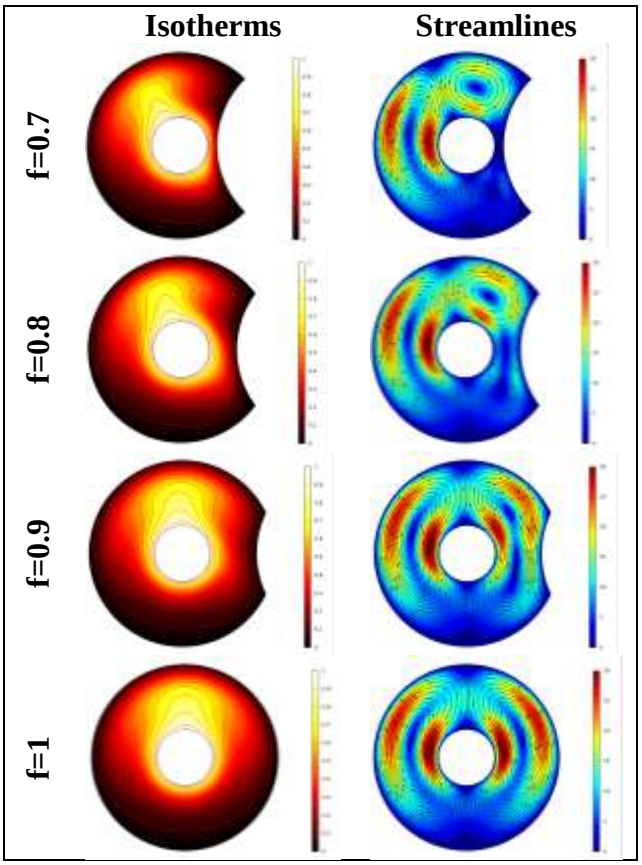

Fig. 23: Isotherms and streamlines for different exterior groove sizes, e=0.3, ϕ0=0°, Ra=1E4

Figure 26 presents the evolution of the heat transfer rate in the form of the average Nusslet number as a function of the position and size of the groove. Note that in the case of weak grooves (f=0.9 and 0.8), the process provides almost the same heat transfer rate as that in the absence of groove (f=1) with a slight decrease on the interval (-40°,90°) for f=0.9 and a slight increase on the interval (-90°,60°) for f=0.8.

By increasing the size of the groove at f=0.7, we notice a crucial increase of about 31% in the rate of heat transfer between the two pipes, with a very small decrease noted on the interval (-50°,50°).

The study of the energy efficiency of the thermal process shown in Figure 27 shows that small grooves (f=0.9) are as efficient as the non-grooved pipes. On the other hand, as the groove gets deeper, the energy efficiency of the system starts to decrease, especially when the groove size exceeds f=0.7. The maximum drop is around 34% when using a grooved pipe of size f=0.7 in position ϕ_0=90°.

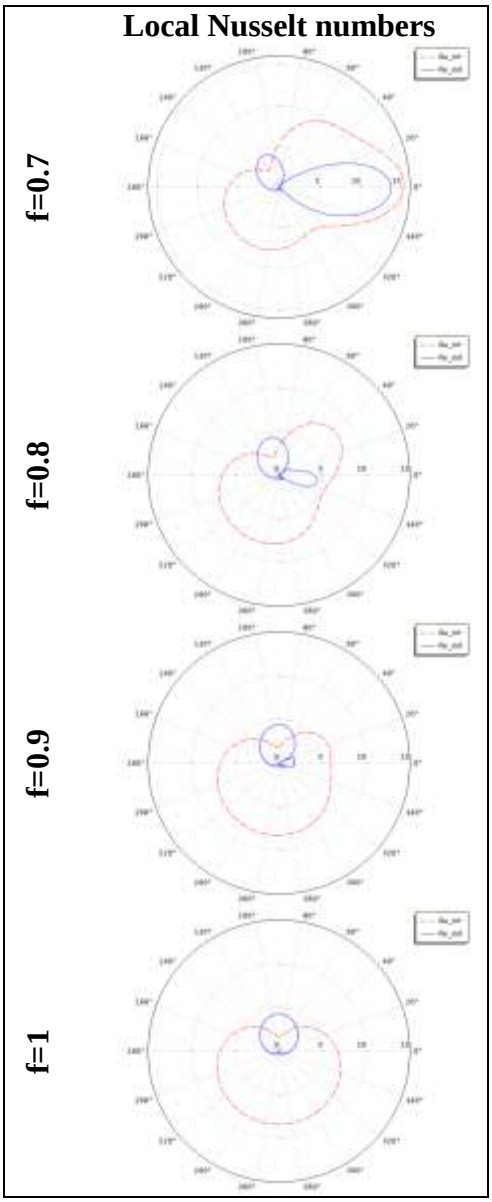

Fig. 24: Evolution of local Nusselt numbers for different exterior groove sizes, e=0.3, ϕ_0=0°, Ra=1E4

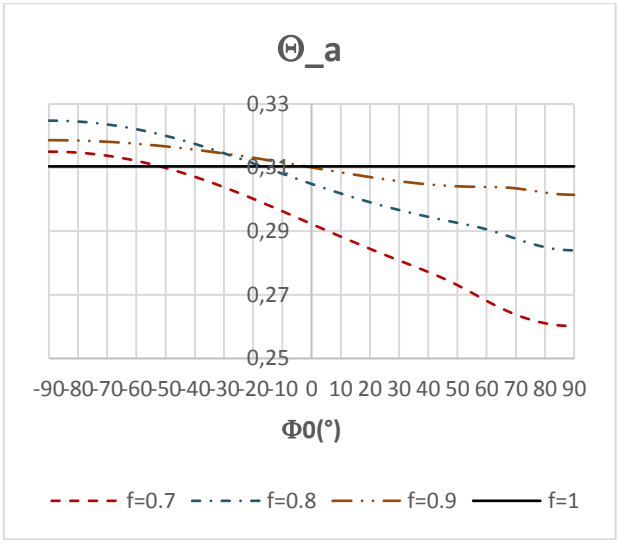

Fig. 25: Effect of groove sizes on the mean dimensionless temperature for the case of exterior groove

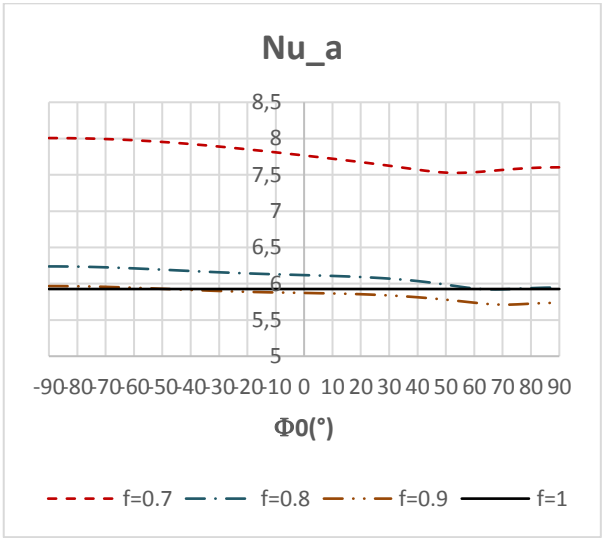

Fig. 26: Effect of groove sizes on the average Nusselt number for the case of exterior groove

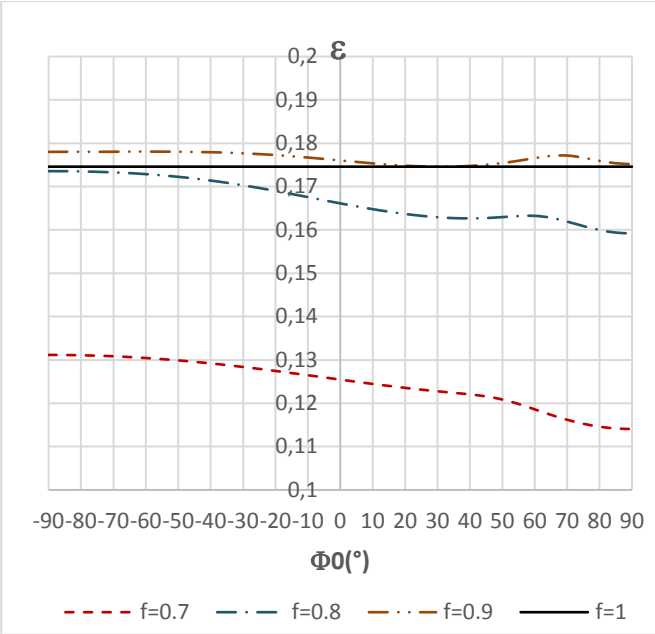

Fig. 27: Effect of groove sizes on the energy efficiency of the process for the case of exterior groove

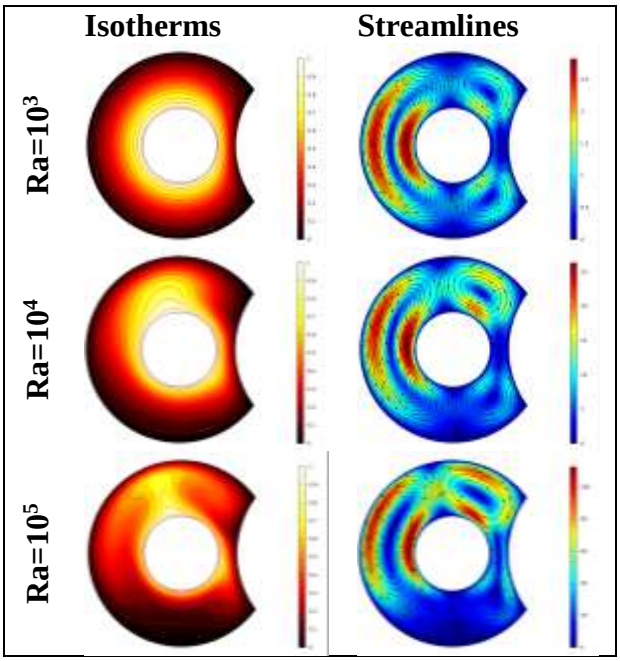

Fig. 28: Isotherms and streamlines for different Rayleigh numbers for the case of exterior groove, e=0.3, ϕ0=0°, Ra=1E4

3.2.3 Effect of Rayleigh Number

The effects of Rayleigh number on the evolution of temperature, fluid flow and local Nusselt number in the annular space are reported in Figure 28 and Figure 29 respectively. The mentioned profiles do not show any symmetry because of the presence of the groove on the right side and the fixed boundary conditions. The fluid flow follows two rotating cells and the right cell contains two secondary recirculation due to the presence of the groove. At low Rayleigh number $Ra=10^3$, the heat is exchanged purely by conduction through the thick thermal boundary layers developed around the hot cylinder. The Nusselt number values are then low and improved slightly at the vicinity of the groove where the temperature gradient is higher.

It should be noted here that the thermal plume starts to appear with $Ra=10^4$ and it amplifies further with $Ra=10^5$. At this stage, the convective heat transfer with the exterior cylinder is then dominant and reaches its maximum value at the plume level. In addition, the circulation of fluid particles accelerates especially on the upper right cell and leads to an improvement of the heat transfer rate with the inner cylinder. This also leads to the appearance of an immobile fluid zone on the lower part of the space and reduces the heat transfer rate with the outer cylinder.

The variation of the average dimensionless temperature as a function of the groove position is shown in Figure 30 for different Rayleigh numbers. We note that, at a low Rayleigh number, the position of the groove does not affect the average temperature of the fluid particles since the transfer is conductive. On the other hand, when the natural convection becomes dominant, ($Ra=10^4$, 10^5), we notice that the effect of the position of the groove becomes considerable and is amplified by increasing the Rayleigh number. Noteworthy for the case $Ra=10^4$, is that for groove positions lower than 5 degrees, the temperature of the fluid increases compared to its values with $Ra=10^3$, but they decrease when the groove is placed beyond 5°. The same decreasing profile is noted when increasing Rayleigh to $Ra=10^5$ with a stagnation of temperatures that appears from the position $\phi_0=40°$.

The effect of Rayleigh number on the average Nusselt number is illustrated in Figure 31 for different positions of the groove. According to the curve, the amount of heat exchanged improves by increasing the Rayleigh number, and remains almost constant by changing the position of the groove. On the other hand, according to Figure 32 which demonstrates the effect of the Rayleigh number on the energy efficiency of the thermal system studied, the latter decreases as the Rayleigh number increases and is unaffected by the position of the groove.

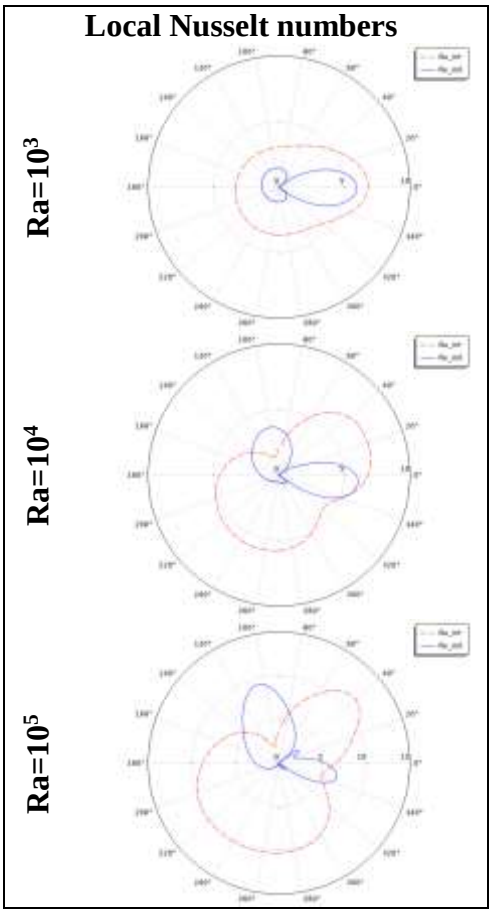

Fig. 29: Evolution of local Nusselt numbers for different Rayleigh numbers for the case of exterior groove, e=0.3, ϕ0=0°, Ra=1E4

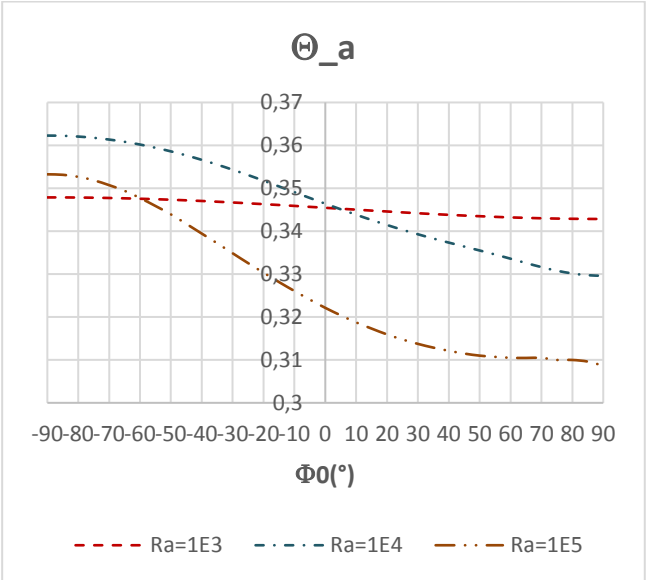

Fig. 30: Effect of Rayleigh number on the mean dimensionless temperature for the case of exterior groove

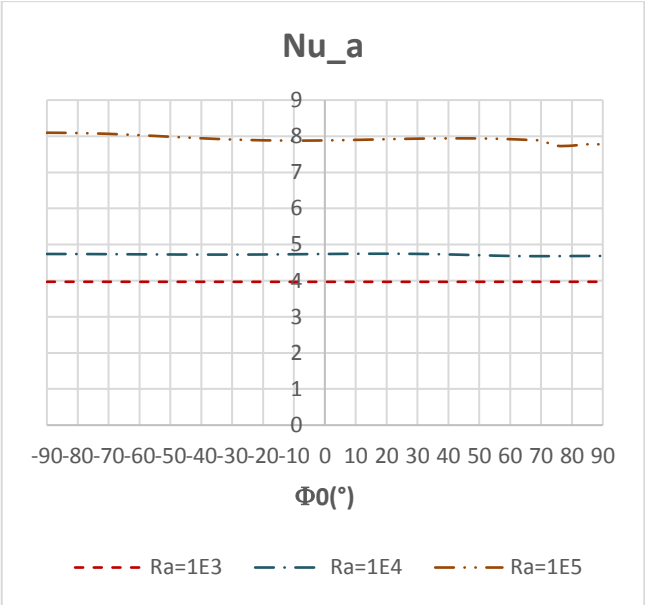

Fig. 31: Effect of Rayleigh number on the average Nusselt number for the case of exterior groove

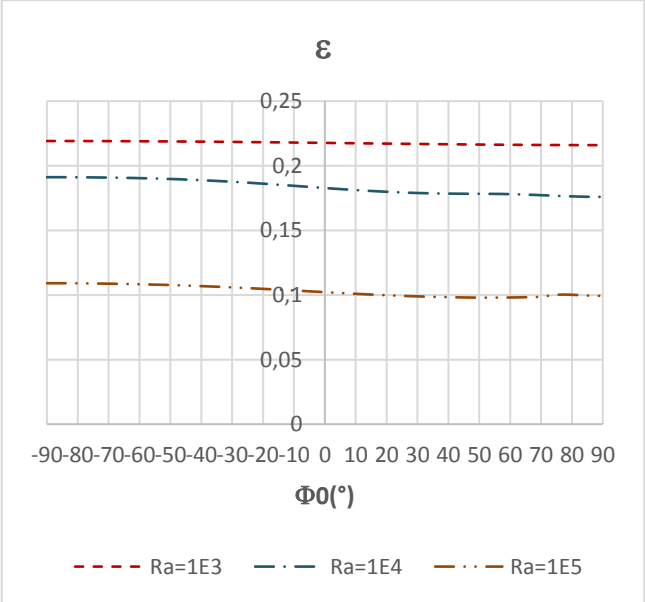

Fig. 32: Figure 5 Effect of Rayleigh number on the energy efficiency of the process for the case of exterior groove

3.2.4 Effect of the Radius Ratio

As an illustration of the aspect ratio effect, the flow and temperature profiles, as well as the local Nusselt number distributions are plotted in Figure 33 and Figure 34 for the case ($Ra=10^4$, f=0.9, $\phi_0=0°$).

We note here that the fluid flow presents two vertical convective cells whose right one contains two secondary cells because of the presence of the groove. The circulation speed is maximum on the left cell and leads to maximum values of Nu_{in} on this side. The heat transfer rate with the outer

cylinder also reaches maximum values at the level of the thermal plume which propagates above the hot cylinder, and at the level of the groove where the thermal gradient is high. By increasing the radius ratio, the heat exchange surface decreases, and the circulation speed drops, causing a decrease in the heat transfer rate with the interior pipe. On the other hand, the exchange space on the right side is more reduced due to the presence of the groove. This induces an increase in temperature gradient and subsequently an increase of heat transfer rate with the outer pipe.

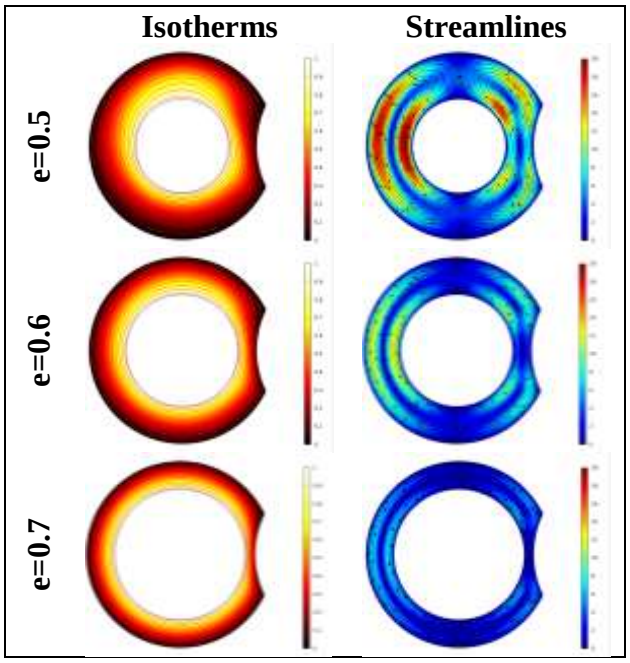

Fig. 33: Isotherms and streamlines for different radius ratios for the case of exterior groove, e=0.3, ϕ0=0̊, Ra=1E4

The impact of radius ratio e on the dimensionless mean temperature of fluid particles as well as on the mean Nusselt number is signaled in Figure 35 and Figure 36. The results found are obvious since the reduction of the exchange surface causes a drop in the heat transfer rate and an aggravation of the average temperature of the domain. Furthermore, as shown in Figure 37, the energy efficiency remains constant as a function of the groove position at high radius ratios (e=0.7), and it starts to show a decreasing trend over the interval [-50̊,30̊] for e<0.7 with an increasing slope as e decreases.

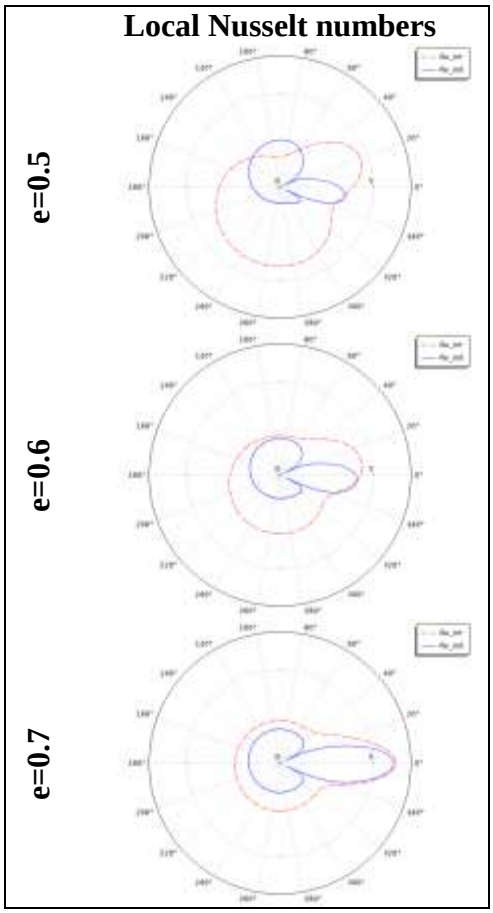

Fig. 34: Evolution of local Nusselt numbers for different radius ratios for the case of exterior groove, e=0.3, ϕ_0=0̊, Ra=1E4

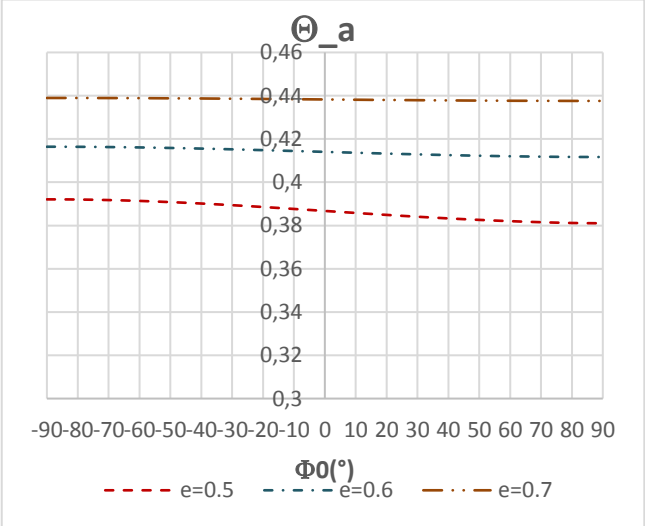

Fig. 35: Effect of radius ratio on the mean dimensionless temperature for the case of exterior groove

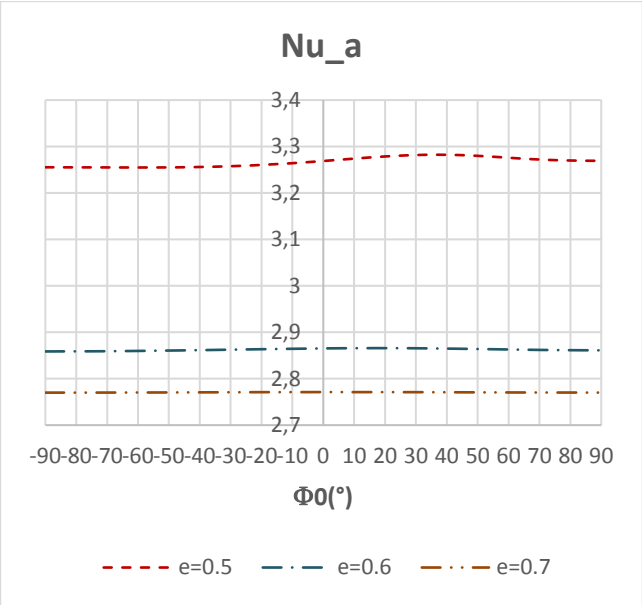

Fig. 36: Effect of radius ratio on the average Nusselt number for the case of exterior groove

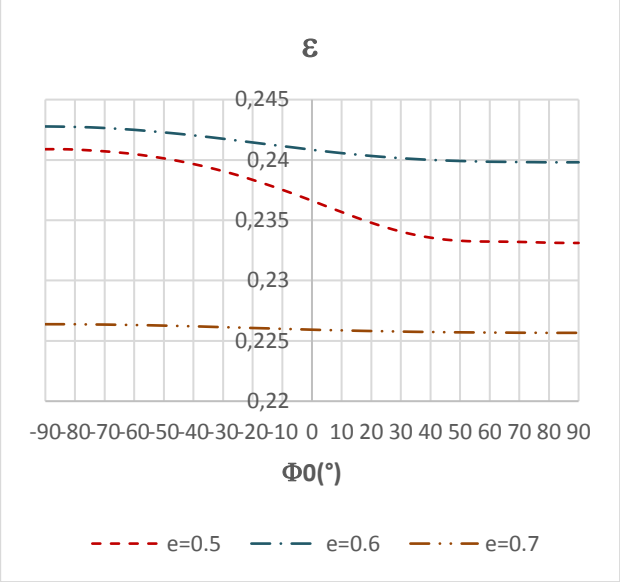

Fig. 37: Effect of radius ratio on the energy efficiency of the process for the case of exterior groove

4 Discussion

The results of the numerical simulation show that increasing Rayleigh number leads to an amelioration of the heat transfer rate. However, the energy efficiency of the process decreases for both inner and outer grooves. So, to keep better energy efficiency, it is recommended to maintain a lower Rayleigh number in the grooved annulus.

The effect of groove position ϕ_0 on the local heat transfer rate was studied for the case of interior groove and exterior groove respectively. One can remark that if the groove is on the interior pipe, then the amount of heat locally exchanged is not affected by the position of the groove. Furthermore, the heat transfer and the energy efficiency are maximum at ϕ_0=40° and ϕ_0=90° respectively. However, when the exterior pipe is grooved, it is essential to choose the position of the groove well according to the need for heat exchange, because it has been found that it is very much affected by the position of the groove.

In addition, by analyzing the effect of groove size and comparing it to the case of non-grooved annulus, it is found that; when the groove size increases, the heat transfer rate for the inner grooved annulus decreases well, however its energy efficiency increases. So in this configuration, it is important to identify the aim of the use of grooved annulus. If the aim is to boost the heat transfer rate, the users have to think about eliminating the groove completely or reducing the size of the groove as much as possible. If the objective of using grooved annulus is to improve cooling or to boost the energy efficiency of the process, then in this case the size of the groove will have to be increased.

It is also found that the mean temperature of the fluid particles in the annulus is decreasing with the increase of the size of the groove. Therefore, if the main function of the industrial process is to maintain the lowest possible fluid temperature, then it will be necessary to opt for bigger grooves. However, to avoid the effect of the presence of the groove, and to have a thermal behavior identical to that in an ungrooved annulus, it is recommended to place the groove at an angle ϕ_0=65°.

In addition, it is found that; in the case of interior groove; increasing the radius ratio e (i.e. decreasing the annulus area) contributes to an amelioration of the energy efficiency of the process, which remains almost constant regardless of the groove location ϕ_0.

On the other hand, for the case of exterior grooved annulus, the heat transfer rate is almost equal to that of non-grooved annulus for f<0.7. We note also a decrease of 34% of the energy efficiency with the increase of the size of the groove to f=0.7 at ϕ_0=90°. Moreover, for cooling applications, it should increase the surface of the annulus (low radius ratio e) to maximize the heat transfer rate whatever the groove location.

5 Conclusion

This work deals with a numerical analysis of the natural convection heat transfer in grooved

cylindrical annulus. The inner cylinder is hot and the outer one is cold. Two types of groove are studied: inner groove for the case where the groove is located on the inner cylinder, and exterior groove if the outer cylinder is grooved. The numerical simulations were conducted using COMSOL Multiphysics® software.

Effects of Rayleigh number, groove locations, groove size and radius ratio of the annulus on the heat transfer rate and energy efficiency of the grooved annulus were investigated. Their effects on the evolutions of dimensionless temperature and velocity were also carefully analyzed for both cases of inner groove and exterior groove. In the light of the simulation results, it was found that the heat transfer rate is maximum when the inner groove is located at ϕ_0=40°, whatever the groove size. Furthermore, the energy efficiency of the process increases with the inner groove size and it is maximum when the inner groove is positioned at ϕ_0=90°. In addition, it was found that the thinner the annular space, the more efficient the process, and the lower the amount of heat exchanged when the inner pipe is grooved. However, for the case of exterior groove, the energy efficiency decreases well with the increase of the size of the groove.

Finally, in this work, we have evaluated the thermal and dynamic behavior in grooved annulus. Highlighting the effect of inner and outer groove on the energy efficiency of the process was an asset of this work, and would be very useful for manufacturers to manipulate the grooved pipes, and choose the position and intensity of the groove that suits their needs. However, evaluating the natural convection heat transfer for the case of double grooved annulus that contains grooves on both inner and outer ducts was not treated in this work, and it would be interesting to meet the needs of multiple engineering applications.

Nomenclature

e	radius ratio
f	groove size
g	acceleration due to gravity [m·s^{-2}]
L	total length of the grooved surface
Nu	Nusselt number
P	pressure [Pa]
Pr	Prandtl number
R	cylinder radius [m]
Ra	Rayleigh number
(r,θ)	cylindrical coordinate system
T	temperature [K]
ΔT	temperature difference, $T_h - T_c$ [K]
(U,V)	dimensionless velocity components
(u,v)	velocity components [m·s^{-1}]
W	dimensionless angular velocity
(X,Y)	dimensionless Cartesian coordinates
(x,y)	cartesian coordinates

Greek Symbols

α	thermal diffusivity [m^2·s^{-1}]
β	thermal expansion coefficient [K^{-1}]
ε	energy efficiency
Θ	dimensionless temperature
ν	kinematic viscosity [m^2·s^{-1}]
Π	dimensionless pressure
ρ	density [kg·m^{-3}]
ϕ_0	groove location

Subscripts

a	average
c	cold
h	hot
ex	exterior
in	interior

References:

[1] Macha_c, I., Dole_cek, P., Macha_cov_a, L., Poiseuille flow of purely viscous non-Newtonian fluids through ducts of non-circular cross section. *Chem. Eng. Process* 38, 1999, pp. 143–148.

[2] McEachern, D.W., Axial laminar flow of a non-Newtonian fluid in an annulus. *AIChE J.* 12 (2), 1966, pp. 328–332.

[3] David, J., Filip, P., Explicit solution of laminar tangential flow of power-law fluids in concentric annuli. *Acta Technica CSAV* 39, 1994, pp. 539–544.

[4] Kumar R., Study of natural convection in horizontal annuli. *Int J Heat Mass Transf.* 31,1988, pp. 1137–48.

[5] R.E. Powe, C.T. Carley, E.H. Bishop, Free convective flow patterns in cylindrical annuli, *J. Heat Transfer* 91, (1969), pp. 310-314.

[6] T. H. Kuehn and R. J. Goldstein, An experimental and theoretical study of natural convection in the annulus between horizontal concentric cylinders, *J. Fluid Mech*. 74, (1976), pp. 695-719.

[7] T. H. Kuehn and R. J. Goldstein, An experimental and theoretical study of natural convection in the annulus between horizontal concentric cylinders, J. Fluid Mech. 74, 1976, pp. 695-719.

[8] Haciislamoglu, M., Langlinais, J., Non-Newtonian fluid flow in eccentric annuli, *ASME Energy Resources Conference and Exhibition*, New Orleans, 1990, pp. 115–123.

[9] Hussein, Q.E., Sharif, M.A.R., Viscoplastic fluid flow in irregular eccentric annuli, *J. Energy Res. Tech.* 120, 1997, pp. 201–207.

[10] Wang, Y., Axial flow of generalized viscoplastic fluids in noncircular ducts, *Chem. Eng. Commun* 168, 1998, pp. 13–43.

[11] Desrayaud G., Lauriat G., Cadiou P. Thermoconvective instabilities in a narrow horizontal air-filled annulus, *International Journal of Heat and Fluid Flow, vol.* 21(1), (2000), pp.65–73.

[12] C. Shu, L. Wang, Y.T. Chew, N. Zhao, Numerical study of eccentric Couette–Taylor flows and effect of eccentricity on flow patterns, *Theoret. Comput. Fluid Dynamics, vol.* 18, 2004, pp. 43–59.

[13] Kan Qin, Daijin Lia, Chuang Huanga, Yubiao Sunb, Jianyong Wangc, Kai Luoa, Numerical Investigation on Heat Transfer Characteristics of Taylor Couette Flows Operating with CO2, *Applied Thermal Engineering*, 2019, Vol. 165, 25, January 2020, 114570.

[14] D.N. Mahony, R. Kumar, E.H. Bishop, Numerical investigation of variable property effects on laminar natural convection of gases between two horizontal isothermal concentric cylinders, *ASME Journal of Heat Transfer,* vol. 108 (1986), pp. 783–789.

[15] J.D. Chung, C.J. Kim, H. Yoo, J.S. Lee, Numerical investigation on the bifurcative natural convection in a horizontal concentric annulus, *Numerical Heat Transfer, Part A: Applications*, vol.36 (1999), pp. 291–307.

[16] J.S. Yoo, Dual free-convective flows in a horizontal annulus with a constant heat flux wall, *International Journal of Heat and Mass Transfer*, vol. 46 (2003), pp. 2499–2503.

[17] U. Projahn, H. Beer, Prandtl number effects on natural convection heat transfer in concentric and eccentric horizontal cylindrical annuli, *Heat and Mass Transfer*, vol.19 (1985), pp. 249–254.

[18] F. Shahraki, Modeling of buoyancy-driven flow and heat transfer for air in a horizontal annulus: effects of vertical eccentricity and temperature-dependent properties, *Numerical Heat Transfer, Part A: Applications*, vol. 42 (2002), pp. 603–621.

[19] M.M. Elshamy, M.N. Ozisik, J.P. Coulter, Correlation for laminar natural convection between confocal horizontal elliptical cylinders, *Numerical Heat Transfer, Part A: Applications*, vol. 18 (1990), pp. 95–112.

[20] H. Asan, Natural convection in an annulus between two isothermal concentric square ducts, *International Communications in Heat and Mass Transfer*, vol. 27 (2000), pp.367–376.

[21] Xu Xu, Gonggang Sun, Zitao Yu, Yacai Hu, Liwu Fan, Kefa Cen, Numerical investigation of laminar natural convective heat transfer from a horizontal triangular cylinder to its concentric cylindrical enclosure, *International Journal of Heat and Mass Transfer*, vol. 52 (2009), pp.3176–3186

[22] Canpolat, C., Characteristics of flow past a circular cylinder with a rectangular groove. *Flow Meas. Instrum*., 2015, 45, 233–246.

[23] Canpolat, C., Sahin, B., Influence of single rectangular groove on the flow past a circular cylinder. *Int. J. Heat Fluid Flow* 64, 2017, 79–88.

[24] Atakan Tantekin , N. Filiz Tumen Ozdil, Hüseyin Akilli, Meltem Caliskan, Flow investigation of circular cylinder having different cavities in shallow water, *International Journal of Heat and Fluid Flow* 90 (2021) 108832.

[25] Khaoula Ben Abdelmlek, Faycal Ben Nejma, Impact of grooved cylinder on heat transfer by natural convection in cylindrical geometry, *Advances in Mechanical Engineering*, 2022, Vol. 14(8) 1–16.

[26] Khaoula Ben Abdelmlek, Fayçal Ben Nejma, Numerical analysis of the improving thermal energy efficiency of taylor-couette flow, *WSEAS Transactions on Applied and Theoretical Mechanics*, volume 15, 2020, pp. 236-247, https://doi.org/10.37394/232011.2020.15.26.

[27] Khaoula Ben Abdelmlek, Faycal Ben Nejma, Improved Energy Efficiency of Mixed Convection Heating Process in Eccentric Annulus, *Advances in Mechanical Engineering*, 2021, Vol. 13(8) 1–13.

[28] Mazgar Akram, Jarray Khouloud, Hajji Fadhila, Ben Nejma Faycal, Natural Convection in a Horizontal Cylinder with Partial Heating: Energy Efficiency Analysis, *Journal of Thermal Science*, 29(6), 2020, pp. 1531–1550.

Contribution of Individual Authors to the Creation of a Scientific Article (Ghostwriting Policy)

The authors equally contributed in the present research, at all stages from the formulation of the problem to the final findings and solution.

Sources of Funding for Research Presented in a Scientific Article or Scientific Article Itself

No funding was received for conducting this study.

Conflict of Interest

The authors have no conflicts of interest to declare.